03.4

Effect of micro-sized vapor bubbles on heat transfer at different heater temperature rise rate

© A.A. Levin, P.V. Khan

Melentiev Energy Systems Institute of Siberian Branch of the Russian Academy of Sciences, Irkutsk, Russia
E-mail: Lirt@mail.ru

The paper presents the results of an experimental study of the dynamics of boiling of a subcooled liquid flow at heater temperature rise rates from 250 K/s to 19 000 K/s and subcooling level from 23 to 103 K. The effect of temperature conditions on the relative fraction of bubbles smaller than $50\,\mu$m is studied. A significant contribution of microbubbles at deep subcooling of the liquid and high rate of temperature rise of the heater surface was revealed.

Keywords: nucleate boiling, microbubbles, non-steady heating.

High values of specific heat fluxes are typical for heat exchange at boiling of subcooled liquid, which causes its wide application in various devices. A high rate of the surface temperature rise in emergency situations is a challenge for making predictive models to describe unsteady boiling. The effect of the rate of the heat-release surface temperature rise on the heat exchange dynamics and vapor phase evolution is covered by experimental, numerical, and theoretical studies [1–3]. In case of nucleate boiling of subcooled liquids, the accounting for the contribution of the smallest vapor bubbles to heat exchange remains unsolved. On the one hand, as far as the size of an individual bubble decreases, its contribution into the total heat exchange decreases even more significantly; on the other hand, the nucleation frequency is rising and the distance between nucleation centers is reduced. A number of studies indicate that possibility of dissipation of extremely high heat fluxes by using a special boiling mode called „microbubble boiling" [4–6]. The lifetime of an individual bubble is generally pro rata to its size, so experimental observation of the behavior of microbubbles, i.e., bubbles with detachment diameters of about $50\,\mu$m or less, requires the use of high-speed imaging with high spatial and temporal resolution. The purpose of the present work is to experimentally study the characteristics of unsteady boiling of a subcooled liquid flow at the temperature rise rate of the heat-release surface up to 19 000 K/s.

The scheme of the experimental setup is described in detail in [7]. The heater is a steel cylinder with a wall thickness of 1 mm and an outer diameter of 12 mm. The pressure in the channel was 0.29 MPa, the average upward water flow velocity was 0.52 m/s, the subcooling level $\Delta T_{sub} = 23-103$ K and the heater temperature rise rate during pulse heating varied from 250 to 19 000 K/s. Vapor structures were recorded by means of a Phantom V2012 high-speed video camera at 180 000 frames per second with the frame size of 256×256 pixels. The spatial resolution of the imaging was $5.5\,\mu$m per pixel, which allowed us to record bubbles varying in size from $11\,\mu$m with lifetimes above $11\,\mu$s. The heater temperature rise rate $\dot{T}$ was determined based on the comparison of video data of boiling modes, numerical simulation of unsteady heat exchange up to the moment of vapor phase nucleation and the results of measuring the temperature of the inner surface of the heater by means of thermocouples. Error of determination of $\dot{T}$ was 7%.

The same value of superheating of the heater surface above the temperature of the first bubble appearance T_{ONB} in each experiment was taken as a criterion for selecting the time moment for comparison of different realizations of boiling. Figure 1 shows the distribution of the vapor phase at the moment of time t when $T_w = T_{\mathrm{ONB}} + 17$ K at various ΔT_{sub} and $\dot{T}$. It is easy to see that the maximum bubble sizes increase as the initial subcooling of the flow decreases and the rate of surface temperature rise decreases. For a surface superheating degree of $15-20$ K above the nucleation onset temperature, the data on all active nucleation centers were collected from the video, as well as their corresponding nucleation frequency f_b and maximum bubble size D_m. By analogy with the modified RPI- model presented in our work [8], the heat flow Q_b generated by each nucleation center can be represented as the sum of the components causing the evaporation of the initial vapor volume Q_{ei}, the evaporation of the microlayer Q_{eml}, the thermal conductivity of the microlayer Q_{cml}, and the thermal conductivity of the superheated layer Q_{cs}:

$$Q_{ei} = h_{lg}\rho_g \frac{\pi D_m^3}{6} f_b, \qquad (1)$$

$$Q_{eml} = h_{lg}\rho_l \delta_{ml} \frac{\pi D_{ml}^2}{6} f_b, \qquad (2)$$
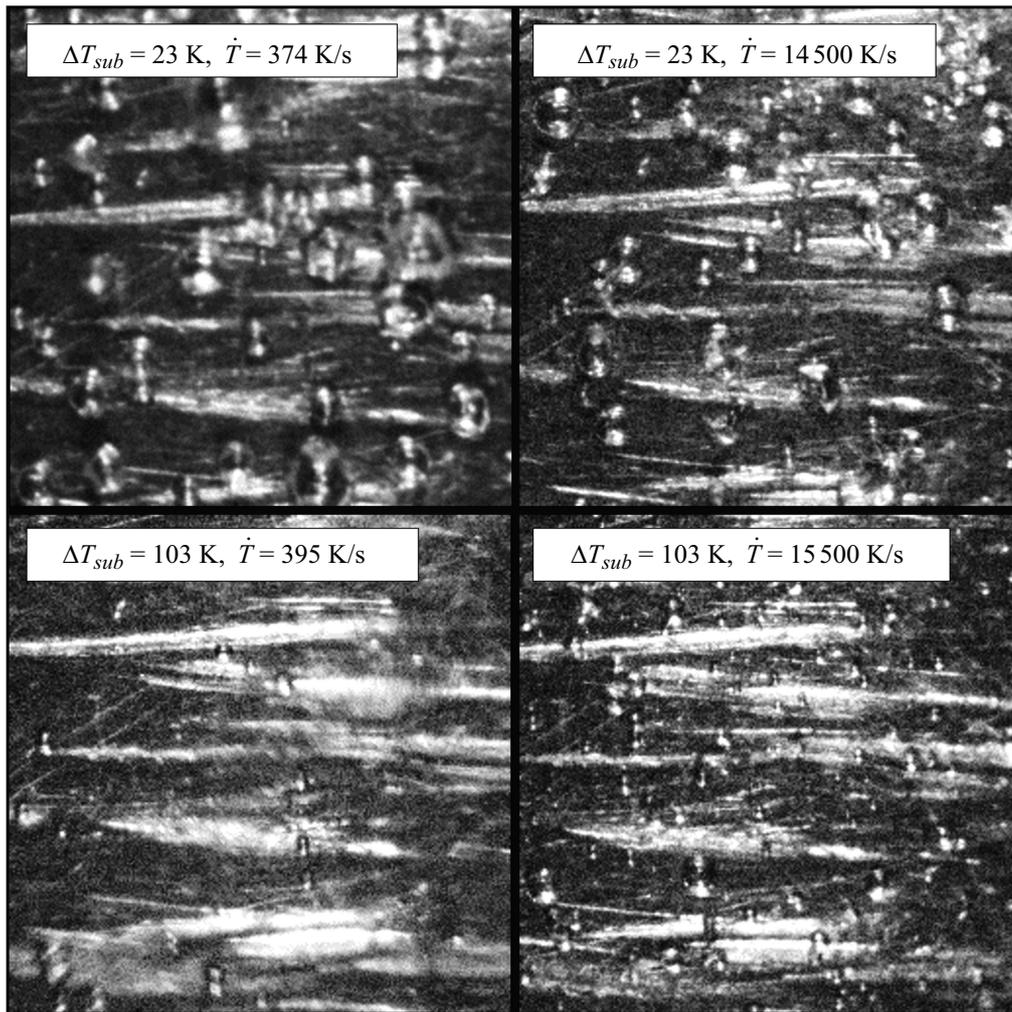
Figure 1. Vapor phase distribution over the heater surface at $T_w = T_{ONB} + 17\,\mathrm{K}$ for different values of liquid subcooling and heater temperature rise rate.

$$Q_{cml} = \frac{\pi k_l (T_w - T_{sat}) D_{ml}^2}{4\delta_{ml}}, \qquad (3)$$

$$Q_{cs} = k_l (T_w - T_{sat}) \pi D_m \left[\ln\left(\frac{\delta_s}{\delta_{ml}}\right) - \frac{2(\delta_s - \delta_{ml})}{D_m} \right]. \quad (4)$$

Here h_{lg} — latent heat of vaporization, ρ_g — saturated vapor density, ρ_l — saturated liquid density, k_l — thermal conductivity of the liquid phase, δ_{ml} — thickness of the microlayer, D_{ml} — diameter of the microlayer, T_w — surface temperature, T_{sat} — saturation temperature. The densities of nucleation centers N_a and specific heat flows q_b are obtained as the total number and total heat flow of bubbles in the video frame, related to the frame area $A = 1.98\,\mathrm{mm}^2$. The data were grouped by the maximum sizes of the bubbles $0-50$, $50-100$, $100-150$, $150-200$, $200-250\,\mu\mathrm{m}$. The nucleation densities and the specific heat flows for the groups of bubbles normalized by the total values N_a and q_b calculated using the formulas $(1)-(4)$ are shown in Fig. 2. At a flow subcooling of 23 K (Fig. 2, a,b), the most of the bubbles have sizes from 50 to 150 $\mu\mathrm{m}$. At

such subcooling for low surface heating rate $\dot{T} = 250\,\mathrm{K/s}$, the nucleation density is $N_a = 18.3\,\mathrm{mm}^{-2}$ and specific heat flow is $q_b = 0.82\,\mathrm{MW/m}^2$, whereas for a surface heating rate of 19 000 K/s, the nucleation density was higher ($N_a = 29.5\,\mathrm{mm}^{-2}$) and $q_b = 2.4\,\mathrm{MW/m}^2$. Bubbles smaller than $50\,\mu\mathrm{m}$ were not detected at subcooling of 23 K and a low value of $\dot{T}$, whereas at a high value of $\dot{T}$ they made 9% (Fig. 2, a) and their contribution to heat exchange was 3% (Fig. 2, b). The difference between the quantity of bubbles distributions and the heat flow distributions is due to the fact that the contribution of each bubble to the heat flux grows with the increase of its diameter, which can be easily observed from the formulas $(1)-(4)$. In the case of a high subcooling of the liquid 103 K (Fig. 2, c,d) at $\dot{T} = 400\,\mathrm{K/s}$, the highest number of bubbles has a maximum size of $75\,\mu\mathrm{m}$, $N_a = 10.2\,\mathrm{mm}^{-2}$ and $q_b = 0.47\,\mathrm{MW/m}^2$, whereas at $\dot{T} = 15\,000\,\mathrm{K/s}$, the highest number of bubbles has a maximum diameter of $25\,\mu\mathrm{m}$, the density of nucleation centers $N_a = 107\,\mathrm{mm}^{-2}$ and $q_b = 3.4\,\mathrm{MW/m}^2$. In case
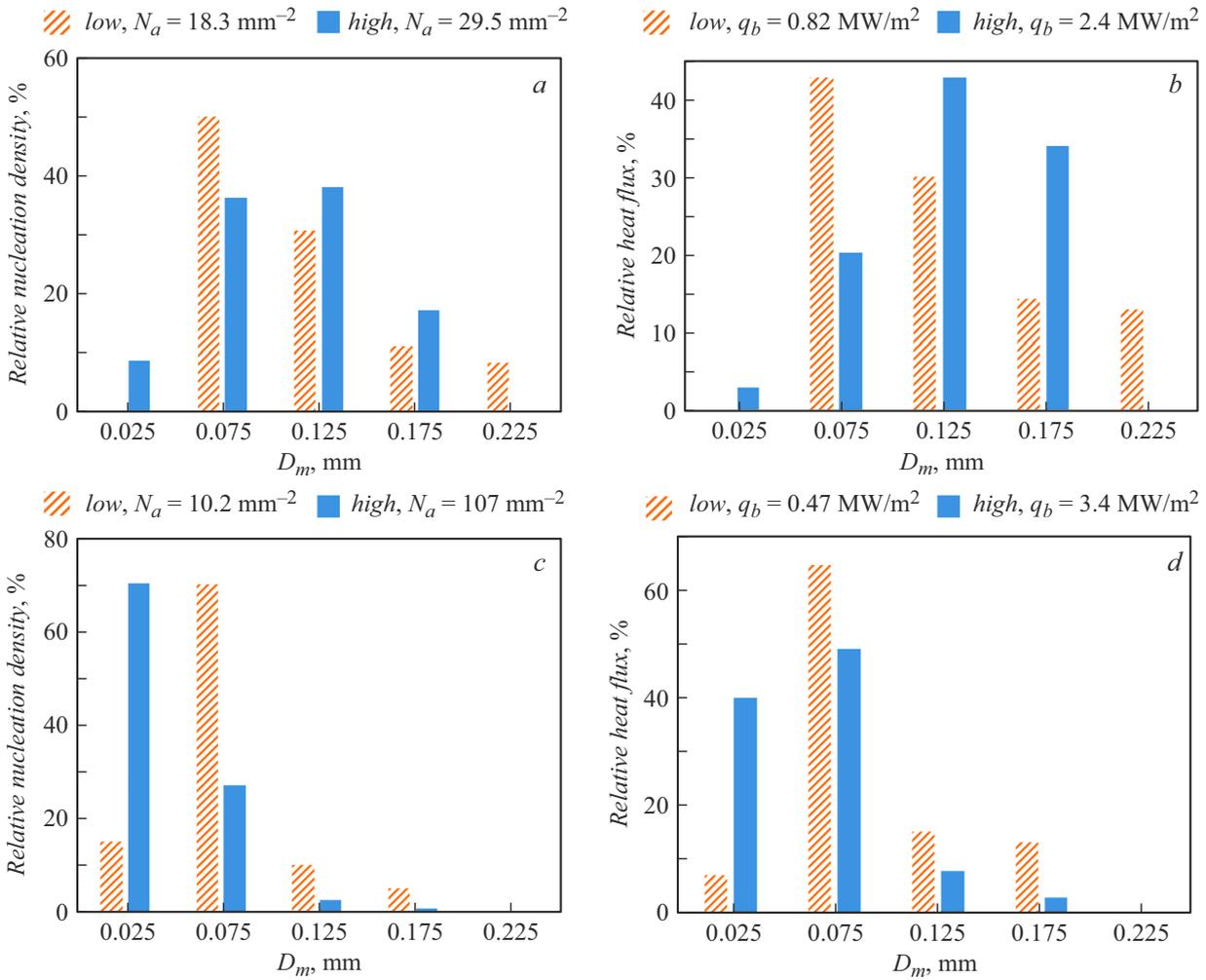
Figure 2. The ratio of the nucleation density of bubble groups to the total nucleation density N_a (a, c) and contribution into the heat flow (b, d) depending on the size of bubbles in case of subcooling of 23 (a, b) and 103 K (c, d) for low $(250-350$ K/s, *low*) and high $(15\,000-19\,000$ K/s, *high*) surface heating rate.
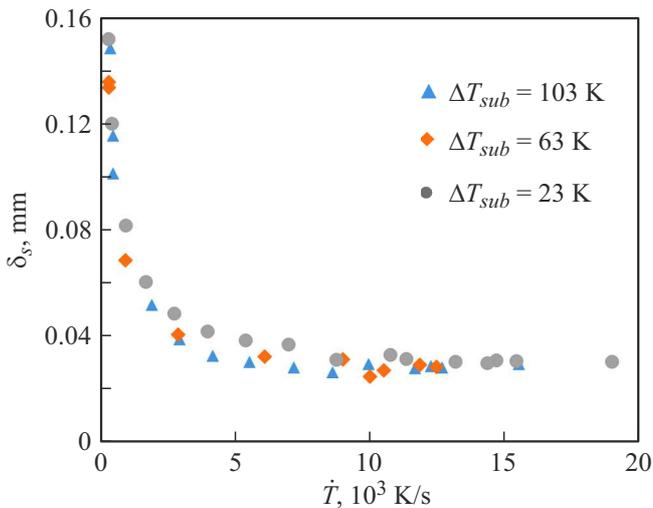
Figure 3. Comparison of calculated values of superheated layer thickness when the heater surface is superheated by 17 K above the nucleation onset temperature at different values of flow subcooling and heater temperature rise rate.

of a liquid subcooling of 103 K, bubbles with sizes up to 50 μm make up 15% of the total number of bubbles and generate 7% of the heat flow $(1)-(4)$ at low surface heating rate $\dot{T} = 400$ K/s, but make up 70% (Fig. 2, c) and generate already 40% of the total heat flow (Fig. 2, d) at $\dot{T} = 15\,000$ K/s.

The change in the ratio of microbubbles with the change in the surface heating rate is associated with the change in the superheated layer thickness $\delta_s = \sqrt{\alpha(t - t_{sat})}$. The vapor bubbles appear to be partially surrounded by the liquid subcooled to the saturation temperature, so the thickness of the superheated liquid layer δ_s limits the maximum size of these bubbles. The relationship between the maximum bubble size and the superheated layer thickness is discussed in [7,9]. The values of δ_s determined using experimental values of nucleation onset times t_{ONB} and surface temperature rise rate $\dot{T}$ are shown in Fig. 3. It can be noted that the thickness of the superheated layer at a fixed level of superheating above the nucleation onset temperature depends weakly on the subcooling of the flow; in case

of the heater temperature rise increase up to 2500 K/s δ_s decreases by several times, and then goes to the asymptotic value. This explains the absence of microbubbles at low subcooling and low surface temperature rise rate. Thus, the contribution of bubbles with sizes up to 50 μm into heat exchange is significant at high values of flow subcooling and high rate of heater temperature rise and can reach tens of percent of the total heat flow associated with the presence of the vapor phase.

Funding

Conflict of interest

The authors declare that they have no conflict of interest.

References

[1] T. Bar-Kohany, Y. Amsalem, Int. J. Heat Mass Transfer, **126**, 411 (2018). DOI: 10.1016/j.ijheatmasstransfer.2018.05.091
[2] A. Kossolapov, F. Chavagnat, R. Nop, N. Dorville, B. Phillips, J. Buongiorno, M. Bucci, Int. J. Heat Mass Transfer, **160**, 120137 (2020). DOI: 10.1016/j.ijheatmasstransfer.2020.120137
[3] S. Fau, W. Bergez, C. Colin, Exp. Therm. Fluid Sci., **83**, 118 (2017). DOI: 10.1016/j.expthermflusci.2016.12.012
[4] Yu.A. Zeigarnik, K.A. Khodakov, V.L. Nizovskii, Yu.L. Shekhter, High Temp., **47** (5), 675 (2009). DOI: 10.1134/S0018151X09050095.
[5] V.V. Yagov, A.R. Zabirov, M.A. Lexin, Therm. Eng., **62** (11), 833 (2015). DOI: 10.1134/S0040601515110117.
[6] M.A. Lexin, V.V. Yagov, A.R. Zabirov, P.K. Kanin, M.M. Vinogradov, I.A. Molotova, High Temp., **58** (3), 369 (2020). DOI: 10.1134/S0018151X20030116.
[7] A.A. Levin, P.V. Khan, Int. J. Heat Mass Transfer, **124**, 876 (2018). DOI: 10.1016/j.ijheatmasstransfer.2018.03.078
[8] A.A. Levin, P.V. Khan, Appl. Therm. Eng., **149**, 1215 (2019). DOI: 10.1016/j.applthermaleng.2018.12.126
[9] H.C. Ünal, Int. J. Heat Mass Transfer, **19**, 643 (1976). DOI: 10.1016/0017-9310(76)90047-8

Translated by EgoTranslating